Front. Optoelectron. 2019, 12(1): 4–14
https://doi.org/10.1007/s12200-019-0868-7

REVIEW ARTICLE

Joint timing and frequency synchronization in coherent optical OFDM systems

Xinwei DU[1,2,3], Pooi-Yuen KAM[1], Changyuan YU (✉)[3]

1 Department of Electrical and Computer Engineering, National University of Singapore, Singapore 117583, Singapore
2 National University of Singapore (Suzhou) Research Institute, Suzhou 21512, China
3 Department of Electrical and Information Engineering, The Hong Kong Polytechnic University, Hung Hom, Kowloon, Hong Kong, China

Abstract In this paper, we review our joint timing and frequency synchronization algorithms in coherent optical orthogonal frequency division multiplexing (CO-OFDM) systems. We first present a timing estimation method by designing the pattern of the training symbol, whose timing metric has a sharp and clear peak, to ensure accurate timing offset (TO) estimation performance. Then we provide both data-aided (DA) and blind (BL) approaches to estimate the carrier frequency offset (CFO). For the DA algorithm, we utilize the same training symbol structure as the timing estimation does, while for the BL algorithm, we utilize the zero-subcarrier power (ZSP) to achieve full-range CFO estimation. Note that our joint timing and frequency synchronization approaches require only one OFDM symbol, which ensure not only the data transmission efficiency, but also the TO and CFO estimation performance. A modified BL ZSP algorithm is proposed to further improve the CFO estimation performance by taking the power average over a series of OFDM symbols. The effectiveness of the TO estimation algorithm, and both the DA and BL CFO estimation algorithms are verified and demonstrated in both simulations and experiments.

Keywords timing offset (TO), carrier frequency offset (CFO), coherent optical orthogonal frequency division multiplexing (CO-OFDM), zero-subcarrier power (ZSP)

1 Introduction

Coherent optical orthogonal frequency-division multiplexing (CO-OFDM) has been an attractive technology for long-haul optical communication systems, due to its high spectral efficiency and excellent tolerance to the fiber chromatic dispersion (CD) and polarization mode dispersion (PMD) [1–3]. However, CO-OFDM systems are sensitive to the symbol timing offset (TO) and carrier frequency offset (CFO) [4]. Thus, timing and frequency synchronization is a significant step for carrier recovery at the receiver side.

Various approaches for OFDM synchronization are available in the literature by now. The most promising approach is to apply the theory of maximum likelihood (ML) estimation [5,6]. However, many ML approaches need to solve the likelihood function, which are computationally complicated. Other synchronization methods that may not be optimum with respect to any statistical criterion have also appeared, which is easy to implement with low complexity. Here we present a survey of the principal techniques available that are more commonly used.

Timing synchronization aims to find the beginning of the discrete Fourier transform (DFT) window. A large TO can cause severe system performance degradation. To estimate the TO, various approaches have been proposed in the literature for both wireless and optical communications [7–11]. Schmidl and Cox [8] proposed a data-aided algorithm for timing and frequency synchronization, which is commonly used. In Ref. [8], the training symbol is designed to have two identical halves, based on which, a timing metric can be calculated and the TO estimation is the corresponding peak index. However, the timing metric in this method has a plateau which equals to the length of cyclic prefix (CP), and causes large timing estimation errors. In Ref. [9], Minn et al. modify the Schmidl's method by designing the pattern of training symbol with sign difference to get a sharper peak in the timing metric. However, this method has two high side lobes, which will cause severe TO estimation performance degradation under low signal-to-noise ratio (SNR). Park's method

Received June 1, 2018; accepted January 28, 2019

E-mail: changyuan.yu@polyu.edu.hk

[10] utilizes conjugate symmetric sequence which leads to an even sharper peak compared with Minn's method. However, the large sides still exist and the estimation accuracy will be affected significantly when SNR is low. In Ref. [11], inspired by Park's method, we also utilize the conjugate symmetry property and the proposed training symbol structure can achieve more accurate TO estimation and lower side lobes. In addition, the method in Ref. [9] has been further extended and modified to estimate the CFO jointly [12].

Since the OFDM symbol duration is longer than that of a single carrier system, the CO-OFDM system is sensitive to the CFO. The CFO causes the loss of orthogonality between the subcarriers, which introduces the inter-carrier interference (ICI) to the system. The CFO normalized by the subcarrier spacing can be divided into an integral part and a fractional part. In general, the CFO estimation algorithms can be classified into two categories: the data-aided (DA) and blind (BL) algorithms [7,8,12–20]. Schmidl and Cox's method [8] is one of the most classical DA algorithms. In Ref. [8], two training symbols are utilized to estimate the integral part of CFO, which requires exhaustive search, while the fractional part of CFO is obtained by calculating the phase of the correlation between the two identical halves of the first training symbol. To reduce the estimation complexity, a high-power pilot-tone was proposed to be inserted into the middle of the OFDM spectrum [13], which reduces the complexity for integral part estimation, by just counting the shifted positions of the pilot-tone. In Ref. [14], the training symbol is composed of several identical blocks; the fractional part of the CFO is obtained by using the sample procedure as in Schmidl's method, while the integral part of the CFO is obtained by direct calculations rather than by doing a search. To ensure the CFO estimation stability under poor SNR conditions, in Ref. [15], the training symbol design is done in the frequency domain, and contains several data blocks. The CFO estimate is obtained via a two-step iterative operation in order to achieve better CFO estimation accuracy. In general, an overhead is usually inserted before each OFDM frame for DA algorithms, which reduces the effective data transmission rate. Blind CFO estimation algorithms solves this problem, but may cost more computational complexity. In Ref. [7], the CP was applied to estimate the CFO blindly, whose estimation performance is highly dependent on the length of CP. A guard band power detection (GPD) method is proposed in Ref. [16] to quickly find and correct the integral part of CFO by detecting the power variation of virtual subcarrier. Nevertheless, the sensitivity to the power variation caused by the ICI and background noise is the main drawback. In Ref. [17], a modified GPD algorithm is obtained by designing the training patterns and averaging the subcarrier power. However, both the conventional and modified GPD algorithms are only applicable to the estimation of the integral part, without considering the fractional part.

In this paper, we review our proposed algorithms for joint timing and frequency synchronization. The timing synchronization is first presented by designing the training symbol structure to achieve the sharper main peak in the timing metric [11,12]. Then after the TO compensation, we show both DA and BL algorithms [12,18] for CFO estimation, while the proposed DA CFO estimation algorithm utilizes the same training symbol as that of the TO estimation. We will also present a new modified blind CFO estimation algorithm based on the zero-subcarrier power (ZSP), by averaging the ZSP through a series of symbols. The effectiveness of our proposed and modified algorithms is verified through both simulations and experiments.

2 Signal model

The n-th received time-domain OFDM sample with the appearance of TO, CFO and laser phase noise (LPN) is given by [1]

$$r(n) = x(n-\tau) \otimes h(n) e^{j\left[\frac{2\pi\epsilon n}{N} + \theta(n)\right]} + w(n), \qquad (1)$$

where we have $n = 0,1,...,N-1$. Term N is the number of subcarriers and $x(n)$ is the-th transmitted OFDM sample. Term τ is the TO in the units of sample period (T_s), $h(n)$ is the channel impulse response, and $w(n)$ is the complex additive white Gaussian noise (AWGN) with mean 0 and variance σ^2 . $\otimes$ denotes the convolution operation and ϵ is the normalized CFO which is equal to the value of actual CFO normalized by the OFDM subcarrier spacing, and can be divided into an integral part and a fractional part. The LPN, represented by $\theta(n)$, is a Wiener process, modeled by [1]

$$\theta(n) = \theta(n-1) + v(n), \qquad (2)$$

where $v(n)$ is a Gaussian random variable with mean 0 and variance σ_p^2 . We have $\sigma_p^2 = 2\pi\Delta\nu T$, where $\Delta\nu$ is the combined laser linewidth (CLW) and T is the OFDM sample time interval.

3 Methodology: timing synchronization

In this section, before we proceed to the proposed timing estimation algorithm, let us briefly describe the TO estimation methods presented in Refs. [8–10], i.e., Schmidl's, Minn's and Park's methods.

3.1 Schmidl's method

In Schmidl's method, the training symbol is designed to contain two identical halves, which is shown as follows [8]:

$$P_{\text{Sch}} = [A_{N/2}A_{N/2}], \tag{3}$$

where $A_{N/2}$ represents the samples of length $N/2$. Then the timing estimate is obtained by finding the peak of the timing metric, which is given by [8]

$$M_{\text{Sch}} = |P_1(d)|^2/(R_1(d))^2, \tag{4}$$

where

$$P_1(d) = \sum_{n=0}^{\frac{N}{2}-1} r^*(d+n)r\left(d+n+\frac{N}{2}\right), \tag{5}$$

$$R_1(d) = \sum_{n=0}^{\frac{N}{2}-1} \left|r\left(d+n+\frac{N}{2}\right)\right|^2. \tag{6}$$

The timing metric of Schmidl's method has a plateau which is sensitive to the AWGN and leads to some uncertainty regarding the starting point of the OFDM symbol.

3.2 Minn's method

To alleviate the uncertainty caused by the timing metric plateau and improve the timing estimation accuracy, Minn proposed a modified preamble, which has the following form [9]:

$$P_{\text{Minn}} = [A_{N/4}A_{N/4} - A_{N/4} - A_{N/4}], \tag{7}$$

where $A_{N/4}$ represents a phase noise (PN) sequence of length $N/4$. Then the corresponding timing metric is designed as [9]

$$M_{\text{Minn}}(d) = |P_2(d)|^2/(R_2(d))^2, \tag{8}$$

where

$$P_2(d) = \sum_{m=0}^{1}\sum_{n=0}^{\frac{N}{4}-1} r^*\left(d+\frac{N}{2}m+n\right) r\left(d+\frac{N}{2}m+k+\frac{N}{4}\right), \tag{9}$$

$$R_2(d) = \sum_{m=0}^{1}\sum_{n=0}^{\frac{N}{4}-1} \left|r\left(d+\frac{N}{2}m+n+\frac{N}{4}\right)\right|^2. \tag{10}$$

In Minn's method, the timing metric plateau is eliminated by using negative-values sample at the second-half training symbol, which results in the improvement of the timing estimation performance. However, the peak in Minn's timing metric is a roll off, when SNR is small, the peak may shift to other positions.

3.3 Park's method

To create a sharper timing metric, in Ref. [10], the training symbol is designed to be

$$P_{\text{Park}} = [A_{N/4}B_{N/4}A^*_{N/4}B^*_{N/4}], \tag{11}$$

where $A_{N/4}$ represents the samples of length $N/4$ and $A^*_{N/4}$ is the conjugate of $A_{N/4}$. In addition, $B_{N/4}$ is designed to be symmetric with $A_{N/4}$. Then the timing metric is obtained by utilizing the property of symmetry, which is shown as

$$M_{\text{Park}} = |P_3(d)|^2/(R_3(d))^2, \tag{12}$$

where

$$P_3(d) = \sum_{n=0}^{N/2} r(d-n)r(d+n), \tag{13}$$

$$R_3(d) = \sum_{n=0}^{N/2} |r(d+n)|^2. \tag{14}$$

Park's method can get a sharper peak in the timing metric, however, both Minn's and Park's methods have large side lobes which may cause severe performance degradation at a low SNR.

3.4 Proposed method

To ensure the timing estimation performance, in this subsection, we aims to design the training symbol structure to generate a sharper timing metric and much lower side lobes compared with the conventional methods.

Here, we utilize the property of the conjugate symmetric sequence, and design the training symbol as follows:

$$P_{\text{prop}} = [A_{N/4}, -B^*_{N/4}, -B^*_{N/4}, A_{N/4}], \tag{15}$$

where $A_{N/4}$ represents the time-domain OFDM samples of length $N/4$, B is symmetric with A, and $B^*_{N/4}$ is the conjugate of $B_{N/4}$. P_{prop} is the whole designed training symbol, whose length is N. More specifically, suppose $A_{N/4}$ is composed of four complex samples $[a,b,c,d]$, then the proposed training symbol structure will become: $[a,b,c, d,-d^*,-c^*,-b^*,-a^*,-d^*,-c^*,-b^*,-a^*, a,b,c,d]$.

To suppress the side lobes and get a sharp peak, the proposed timing metric is designed to be the production of two timing metrics. The two timing metrics are actually the correlations between $A_{N/4}$ and $-B^*_{N/4}$, $-B^*_{N/4}$ and $A_{N/4}$, respectively. We can express the proposed timing metric as

$$M(d) = M_1(d)\cdot M_2(d), \tag{16}$$

where

$$M_1(d) = \left|\sum_{n=0}^{\frac{N}{4}-1} r(d-n-1-N/4)r(d+n-N/4)\right| \Big/ \sum_{n=0}^{\frac{N}{4}-1} \left|r\left(d+n-\frac{N}{4}\right)^2\right|, \tag{17}$$

$$M_2(d)=\left|\sum_{n=0}^{\frac{N}{4}-1} r(d-n-1+N/4)r(d+n+N/4)\right| \Big/ \sum_{n=0}^{\frac{N}{4}-1}\left|r\left(d+n+\frac{N}{4}\right)^2\right|. \quad (18)$$

Then the TO estimate $\hat{\tau}$ can be obtained by searching for the d which can maximize the timing metric, i.e.,

$$\hat{\tau}=\text{argmax}_d M(d). \quad (19)$$

4 Methodology: frequency synchronization

In this section, we will give a discussion of our proposed DA and BL CFO estimation algorithms, and for the blind ZSP based algorithm, we propose a new pattern of zero-subcarrier position arrangement to enlarge the ICI caused by the CFO, to further improve the estimation performance.

Here we assume that the phase noise varies slowly so that we can regard it as a constant phase θ within one OFDM symbol, and the TO has been totally compensated. So that Eq. (1) can be simplified as

$$r(n)=x(n)\otimes h(n)\mathrm{e}^{\mathrm{j}[2\pi\epsilon n/N+\theta]}+w(n) \quad (20)$$

After performing the N-point DFT, we have

$$\begin{aligned} R(k)&=\mathrm{e}^{\mathrm{j}\theta}\sum_{n=0}^{N-1} r(n)\mathrm{e}^{-\frac{\mathrm{j}2\pi kn}{N}}+W(k)\\ &=\mathrm{e}^{\mathrm{j}\theta}\sum_{l=-\frac{N}{2}}^{\frac{N}{2}-1}X(l)H(l)\psi_{l-k}+W(k)\\ &=\mathrm{e}^{\mathrm{j}\theta}[X(k)H(k)\psi_0+I_k]+W_k, \end{aligned} \quad (21)$$

where $W(k)$ is the N-point noise spectrum of $w(n)$. Here $X(k)$ and $H(k)$ represent the transmitted signal and the channel transfer function on the k-th subcarrier in the frequency domain, respectively. Term I_k is the ICI caused by the CFO, which can be expressed as [1]

$$I_k=\sum_{l=-\frac{N}{2},l\neq k}^{\frac{N}{2}-1}\psi_{l-k}X(l)H(l), \quad (22)$$

where the ICI coefficient ψ_{l-k} is defined by [1]

$$\psi_{l-k}=\frac{1}{N}\cdot\frac{\sin(\pi(\epsilon+l-k))}{\sin\left(\frac{\pi(\epsilon+l-k)}{N}\right)}\mathrm{e}^{\mathrm{j}\pi(\epsilon+l-k)\left(1-\frac{1}{N}\right)}. \quad (23)$$

4.1 Data-aided CFO estimation algorithm

The proposed DA CFO estimation algorithm utilizes the same training symbol as the timing synchronization step, which can achieve the joint timing and frequency synchronization by utilizing only one OFDM symbol.

Based on the proposed training symbol structure in Eq. (15), for the first half, i.e., $[A_{N/4},-B^*_{N/4}]$, according to the property of conjugate symmetric sequence, the correlations are taken between $r(0)$ and $r(N/2-1)$, $r(1)$ and $r(N/2-2)$, and so on. By similar procedures, the correlation results of the second half can be calculated. We can finally obtain the correlations as

$$\phi_{n,m}=-r\left(n+\frac{mN}{2}\right)r\left(\frac{N}{2}-n-1+\frac{mN}{2}\right), \quad (24)$$

where $m=0,1$ and $n=0,1,...,\frac{N}{4}-1$.

Since the phase difference of two adjacent samples is $2\pi/N$, it indicates that the every product pair in Eq. (12) has phase coefficient $\beta_{n,m}$ which is proportional to $2\pi/N$. Here we give an example for illustration. The phase difference between $r(1)$ and $r(N/2-1)$ is $(N/2-2)2\pi/N$ and the phase difference between $r(N/4-1)$ and $r(N/4)$ is $2\pi/N$, thus the corresponding values of $\beta_{n,m}$ are $\beta_{1,0}=N/2-2$ and $\beta_{N/4-1,0}=1$, respectively. Then the fractional CFO estimate $\hat{\epsilon}_{\mathrm{f}}$ can be obtained as

$$\hat{\epsilon}_{\mathrm{f}}=\frac{2}{N}\sum_{m=0}^{1}\sum_{n=0}^{N/4-1}\frac{\angle\phi_{n,m}}{(2\pi/N)\beta_{n,m}}. \quad (25)$$

As stated in Eq. (20), here we assume the TO has been compensated, the channel is non-dispersive so that $h(n)$ is an impulse, and phase noise varies slowly which can be regarded as a constant phase within one OFDM symbol. Thus under the case of high SNR, the angle of the correlation between the product pairs should be approximately a constant. Because the CFO in the frequency domain actually causes a phase shift in the time domain, which can be seen in Eq. (1) and for the two halves of the training symbol, the summation of the subcarrier index are the same. Here since the phase $\angle\phi_{n,m}$ is independent with and in the presence of only CFO, here we simplify the parameter $\angle\phi_{n,m}$ to $\angle\phi$. Then Eq. (13) can be rewritten as

$$\hat{\epsilon}_{\mathrm{f}}=\frac{2}{N}\frac{\angle\phi}{\sum_{m=0}^{1}\sum_{n=0}^{N/4-1}(2\pi/N)\beta_{n,m}}. \quad (26)$$

To further simplify the computational complexity of Eq. (26), the summation in the denominator can be first obtained by using a given CFO. If $\epsilon=0.1$, by calculating the $\angle\phi$ from the received signal, we can inversely calculate the summation of the phase difference, which can be defined as

$$\alpha=\sum_{m=0}^{1}\sum_{n=0}^{N/4-1}(2\pi/N)\beta_{n,m}. \quad (27)$$

Note that α is a practical value which is also suitable for the estimation of other CFO values, and without the AWGN, the value of α is only related to the value of $\beta_{n,m}$ and N, while $\beta_{n,m}$ is only determined by the training

symbol structure and will not change with the variation of the CFO values. Now we take the AWGN into consideration, since the mean of AWGN variables is 0, $\angle\phi$ is approximated by calculating the mean value of $\angle\phi_{n,m}$. Finally, the CFO estimate can be expressed as

$$\hat{\epsilon}_{\mathrm{f}} = \frac{4}{N^2}\frac{\sum_{m=0}^{1}\sum_{n=0}^{N/4-1}\angle\phi_{n,m}}{\alpha}. \tag{28}$$

The proposed DA CFO estimation algorithm can be used for estimating of the fractional part of CFO, but the integral CFO cannot be obtained. This is because in the time domain, the CFO causes a phase shift, i.e., $\mathrm{e}^{\mathrm{j}2\pi\epsilon n/N}$. In our approach, we take the angle operation which limit the phase range to $[-\pi,\pi]$. By considering the phase difference between $r(0)$ and $r(N/2-1)$, which is $\pi\epsilon-2\pi\epsilon/N$, we can see that if contains an integral part, the obtained phase will be cut to the range of $[-\pi,\pi]$. This means that the proposed DA method can only obtain the fractional part of CFO. To break through this limitation, here the method in Ref. [13] can be applied for the integral part estimation. In Ref. [13], a pilot-tone with high power is inserted in the middle of the OFDM spectrum. Then the estimate of integral part is obtained by just counting the shifted positions of the pilot-tone. The proposed blind ZSP method which will be introduced in the following subsection can also be utilized for estimating the integral part of CFO.

4.2 Blind ZSP-based CFO estimation algorithm

In the frequency domain, the fractional part and the integral part of CFO have difference effects on the received signal. In the presence of fractional CFO, as has shown in Eq. (22), the ZSP increases due to the ICI, while the integral part causes a shift of the amplitude spectrum, which means that the amplitude is no longer symmetric. The effects of CFO on the signal spectrum is investigated in Figs. 1 and 2. In this simulation, the DFT size is 64, with 32 subcarriers carry QPSK modulated data. It is obvious in Fig. 1(a) that the zero-subcarriers (ZSs) are free of power. With the appearance of 0.2 normalized CFO, as shown in Fig. 1(b), the ZSP increases due to the ICI effect. Figure 2(a) verifies that the integral part of CFO causes the shift of spectrum and since in general, the CFO is unknown to the receiver, by still calculating the ZSP at original positions, we can conclude from Fig. 2(b) that when the existing CFO is 0, the ZSP is the minimum. Because by using other CFO values for compensation, the power of zero-subcarriers will increase instead due to the ICI caused by the CFO.

Thus, by utilizing the features stated above, we propose a blind search method for full range CFO estimation. The main idea of the blind ZSP method is to utilize the ICI caused by the CFO, which leads to the power increase of the zero-subcarriers. By compensating the received signal with various possible CFO values, we can finally find the one which leads to the minimum power of zero-subcarriers, i.e., the least ICI. The integral part of CFO is obtained by searching through a series of the normalized CFO candidates:

$$S_i = \left\{\epsilon_p : \epsilon_p = -\frac{N}{2} + p\cdot\Delta\epsilon, p = 0,1,...,N-1, \Delta\epsilon = 1\right\}. \tag{29}$$

In Eq. (30), we first compensate the received time-domain OFDM samples by using the normalized CFO candidate ϵ_p, then the compensated signal is transferred to the frequency-domain by taking the DFT and the total power is calculated by summing the power over all the zero-subcarriers. The estimated integral part is the one that can achieve the minimum ZSP:

$$\hat{\epsilon}_i = \underset{\epsilon_p}{\operatorname{argmin}} \sum_{k\in\{\text{ZS index}\}}\left|\sum_{n=0}^{N-1} r(n)\mathrm{e}^{-\frac{\mathrm{j}2\pi n(\epsilon_p+k)}{N}}\right|^2. \tag{30}$$

After the integral part estimation, the search range can be narrowed down to $[\hat{\epsilon}_i-1,\hat{\epsilon}_i+1]$ to estimate the fractional part. By using the similar procedure, the estimated fractional part of CFO then can be obtained by finding the candidate that achieves the minimum power of zero-subcarriers:

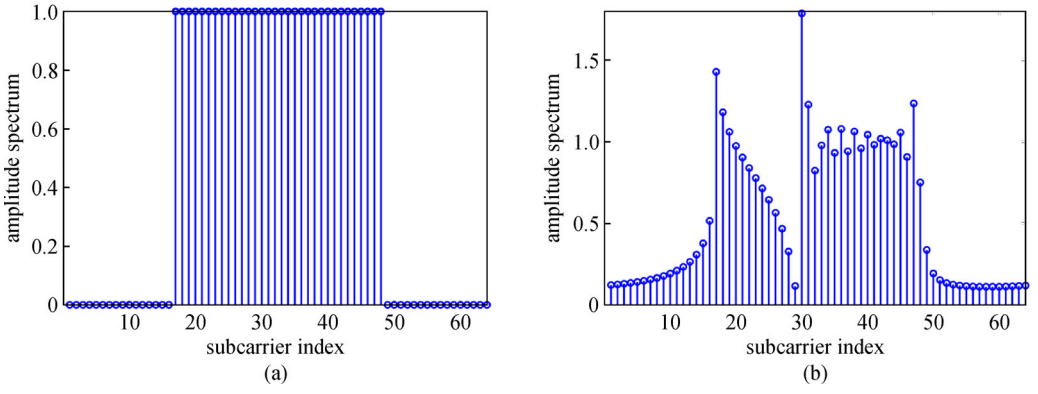

Fig. 1 Amplitude spectrum. (a) Without CFO; (b) with $\epsilon = 0.2$

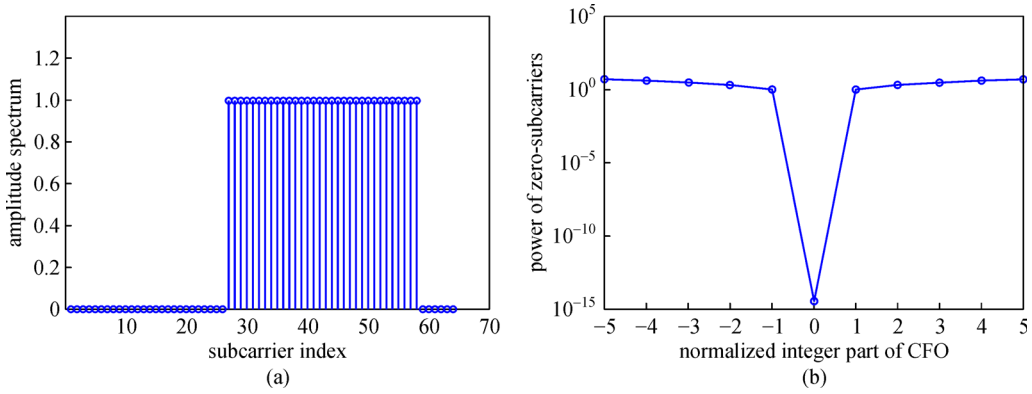

Fig. 2 (a) Amplitude spectrum with $\epsilon = 10$; (b) power of zero-subcarrier vs. various integral CFOs for compensation, with the actual CFO of 0

$$S_f = \left\{ \epsilon_{p'} : \epsilon_{p'} = \hat{\epsilon}_i - 1 + p' \cdot \Delta\epsilon,\ p' = 0,1,...,2M,\ \Delta\epsilon = 1/M \right\}, \tag{31}$$

$$\hat{\epsilon} = \underset{\epsilon_{p'}}{\operatorname{argmin}} \sum\nolimits_{k \in \{\text{ZS index}\}} \left| \sum\nolimits_{n=0}^{N-1} r(n) \mathrm{e}^{-\frac{\mathrm{j}2\pi n(\epsilon_{p'} + k)}{N}} \right|^2. \tag{32}$$

Here $1/M$ is step size and the choice of M is a trade-off between the CFO estimation accuracy and computational complexity.

Since the proposed ZSP algorithm can estimate the CFO by using only one OFDM symbol, when the noise and ICI increase, the estimated CFO will fluctuate around the exact CFO value severely, which leads to the increase of estimation error variance. To achieve a more stable estimation performance, here we modify the algorithm by taking the power average over a number of symbols, and the average power of ZS can be expressed as

$$ZSP_M = \left(\sum\nolimits_{j=1}^{N_s} ZSP_j \right) / N_s. \tag{33}$$

Here, ZSP_j is the power summation of the zero-subcarriers on the j-th OFDM symbol and N_s is the number of OFDM symbols used for CFO estimation. Then based on Eq. (33), we can recalculate the CFO estimate and improve the estimation performance.

The proposed blind method utilizes the power of zero-subcarriers for CFO estimation, which leads to the reduction of spectral efficiency to some degree. However, the CFO estimation performance can be improved with the growing number of zero-subcarriers. It is actually a balance between the spectral efficiency and accuracy.

5 Experimental and simulation results

The OFDM transmitter and receiver diagrams are shown in Figs. 3(a) and 3(b), respectively. The simulations are carried out by using MATLAB and VPI Trasmission-Maker. The pseudo-random binary sequence (PRBS) of length $2^{15}-1$ is generated at the transmitter side, then modulated onto 16 quadrature amplitude modulation (16-QAM). The DFT size is 256, and the length of CP is 8 samples. The number of effective data subcarriers is 123, followed with 5 pilot subcarriers for phase noise estimation. One training symbol is inserted at the beginning of the OFDM frame, which is used for timing and frequency synchronization. For VPI simulation, the sample rate is 20 GSa/s and the laser linewidth is 100 kHz.

For the experiments, the time-domain samples are generated by a 25 GSa/s Arbitrary Waveform Generator to generate I and Q branches of the analog signal first. Then the two branches of analog signal are fed into the IQ modulator, to modulate the signal onto the light and get 16-QAM-OFDM signal. A bias control is applied to find the null point. For timing synchronization, to overcome the effects induced by CFO, we share the same laser source between the transmitter and the local oscillator (LO), whose laser linewidth is 200 kHz operating at 1550 nm. Note that the performance of timing synchronization is

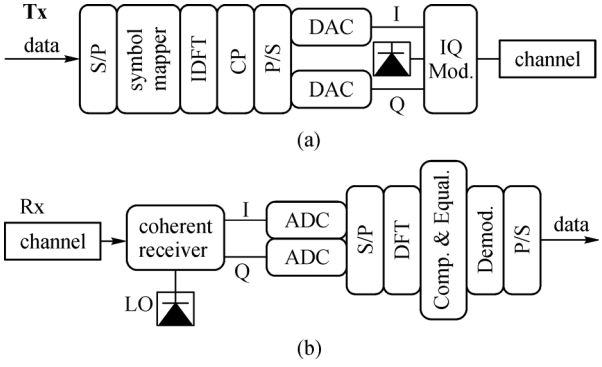

Fig. 3 (a) Transmitter and (b) receiver of a CO-OFDM system. S/P: serial to parallel, CP: cyclic prefix, Mod./Demod.: modulator/demodulator, ADC: analog to digital converter, Comp: compensation, Equal.: equalization, LO: local oscillator

investigated through experiments, while the performance of CFO estimation is based on simulations.

5.1 Timing synchronization

The timing metrics of Schmidl's, Minn's, Park's and the proposed methods are shown in Fig. 4. As can be seen from Fig. 4(a), the timing metric of Schmidl's method has a plateau whose length equals to the length of CP, and is sensitive to the AWGN. Minn's and Park's methods solve this problem, and Park's method has sharper peak than Minn's method. However, both Minn's and Park's methods have large side lobes which may cause severe timing estimation error by finding the wrong peak at low SNR. Compared with these three algorithms, the timing metric of the proposed method shows a clear and sharp peak without any side lobes, even at a low SNR, as shown in Fig. 4(b).

To compare the timing estimation performance of the proposed method with Schmidl's, Minn's and Park's emthods, here in Fig. 5(a), the probability of correct timing estimation is shown. As can be seen Fig. 5(a), Schmidl's method shows the worst timing estimation performance, because the plateau in the timing metric leads to its sensitivity to the AWGN, and can cause severe performance degradation. In addition, since the timing metric of Park's method has a sharper main peak than that of Minn's method, the probability of correct timing estimation of Park's method is higher, especially at low SNR. The proposed method is the best among the four algorithms, whose probability for correct timing estimation can achieve 1 even at −7 dB SNR. The corresponding experimental BER result is shown in Fig. 5(b). It can be observed that Schmidl's method has the worst BER performance, while the proposed method has similar BER performance with Park's method, which is consistent with the simulation results.

5.2 Data-aided CFO estimation

Figure 6 investigates the CFO estimation performance of the proposed DA algorithm, with respect to the estimation error variance and BER performance. In Fig. 6(a), when the optical signal to noise power ratio (OSNR) is lower than 10 dB, the CFO estimation error variance becomes higher when the CFO is larger. However, when the OSNR is above 10 dB, the estimation error variances for various CFOs show the same tendency, which are nearly the same

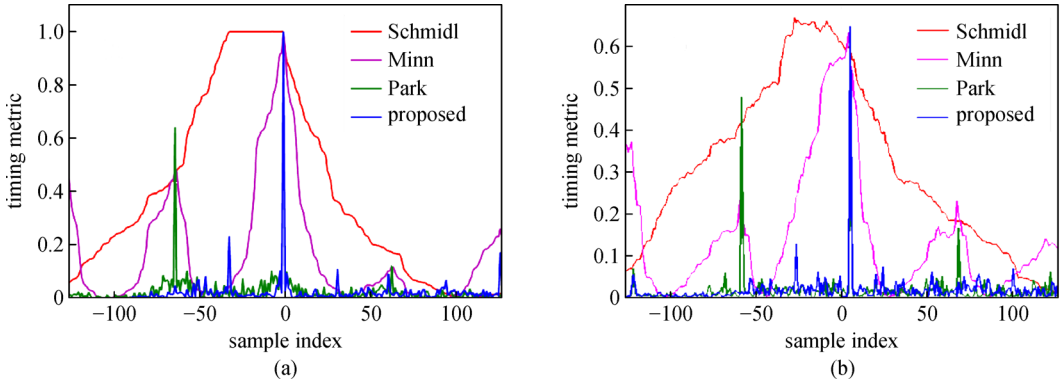

Fig. 4 Timing metrics of Schmidl's, Minn's, Park's and proposed methods, with $\tau = 10$ and (a) no AWGN; (b) SNR = 5 dB

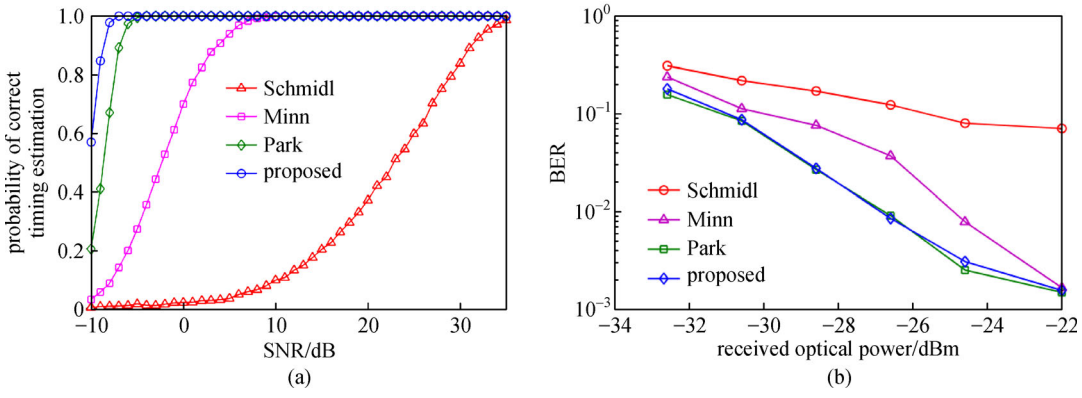

Fig. 5 (a) Probability of correct timing estimation vs. SNR with $\tau = 10$; (b) BER comparison of Schmidl's, Minn's, Park's and the proposed methods vs. received optical power

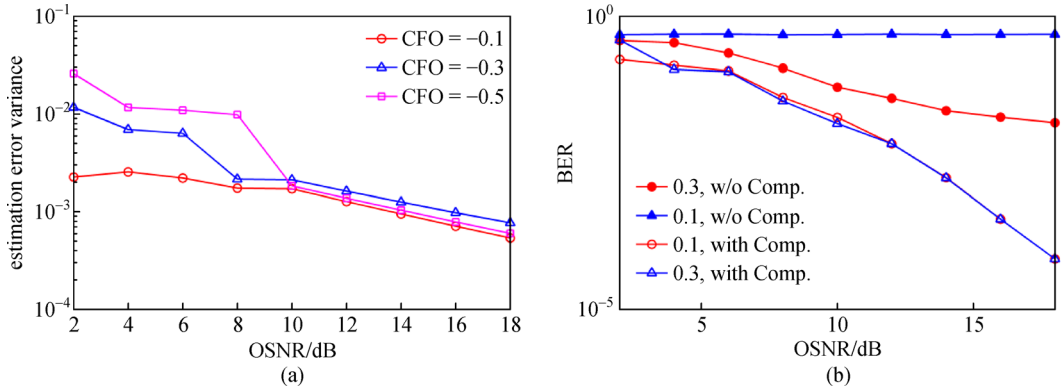

Fig. 6 (a) CFO estimation error variance vs. OSNR under different CFOs; (b) BER vs. OSNR with and without CFO compensation

as each other. In practice, the proposed CFO estimation algorithm may show stable and accurate performance, since for real applications, the OSNR is usually controlled to be higher than 10 dB to ensure the channel quality. In Fig. 6(b), the influence of CFO on the system BER performance is investigated. As can be seen in Fig. 6(b), even though the OFDM signal is only shifted by a very small CFO, the BER performance degrades severely. When the normalized CFO is 0.3 the BER is almost 0.5 at the OSNR of 18 dB, which indicates that the signal is totally distorted. This implies that the CFO has a significant influence on the system performance and the compensation is inevitable and effective to recover the signal.

In Fig. 7, we investigate the feasibility and stability of the proposed DA CFO estimation algorithm with respect to the estimation error variance and the BER performance. The fluctuations in the figure are not obvious except that with 0.5 normalized CFO. This is because the coefficient α is a constant obtained in a perfect condition that the CFO is the only factor that affects the system. However, in the simulations, the LPN appears and the corresponding laser linewidth is 100 kHz. In this case, the value of that utilized for the CFO estimation may not be the optimal one, which happens to cause the minimum estimation error at the CFO of 0.5. Even though the estimation error variance has some fluctuations, the final BER performance will not be affected.

5.3 Blind ZSP-based CFO estimation

In Fig. 8(a), we investigate the CFO estimation error variance vs. the number of symbols (N_s) used for power average, under the SNR of 10 and 15 dB. As can be seen in the figure, a larger number of symbols used for power average can lead to better CFO estimation performance and the variance decreases slowly when the number of symbols is beyond 30. Thus, in the following simulations, we use 30 symbols for power averaging, i.e., N_s= 30. Figure 8(b) demonstrates the effect of the number of zero-subcarriers (ZS). The step size of ZSP method is 1/100. It can be seen that higher estimation accuracy is obtained by the increase of the ZS number, since a larger number of ZS used for calculation leads to more obvious power difference between ZS and other effective data subcarriers. However, the increase of the ZS number will lead to the reduction of spectral efficiency. Moreover, the modified algorithm can significantly improve the system performance to more than

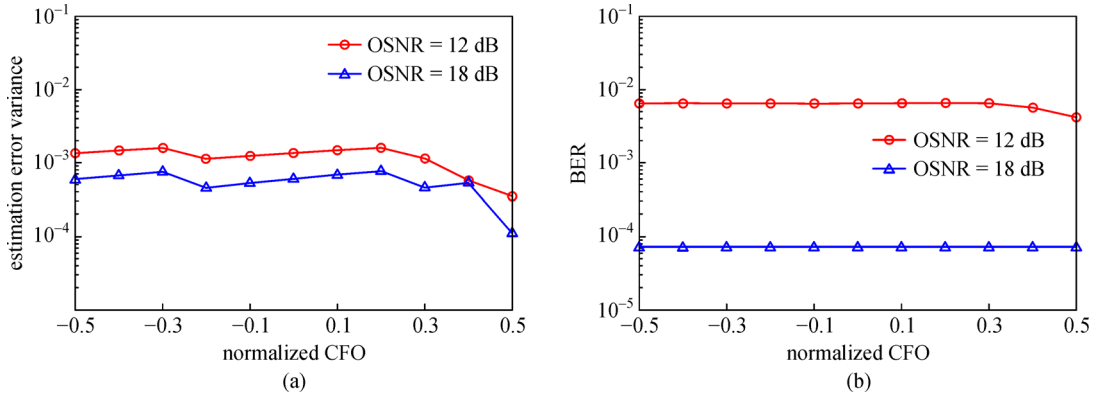

Fig. 7 (a) Estimation error variance vs. normalized CFO under the OSNR of 12 and 18 dB; (b) BER vs. normalized CFO under the OSNR of 12 and 18 dB

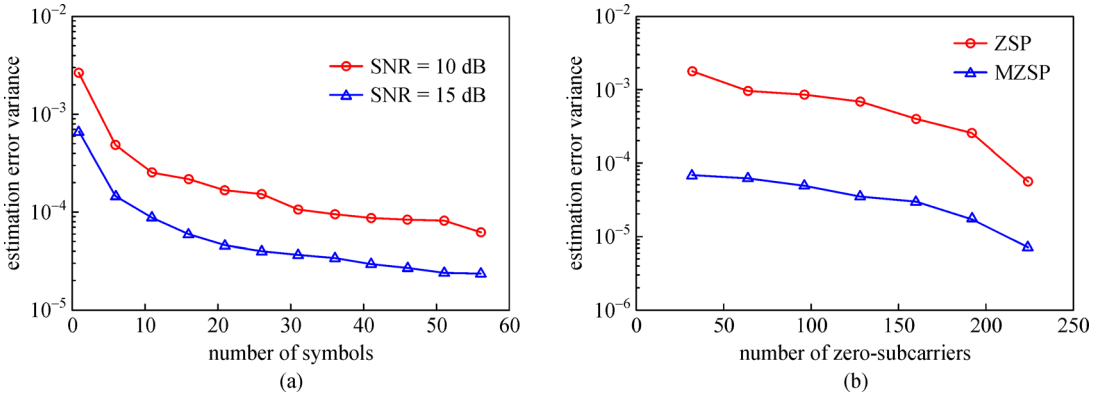

Fig. 8 (a) Estimation error variance vs. the number of symbols used for power average; (b) estimation error variance vs. number of zero-subcarriers, with the CFO of 5 GHz

one order.

Figure 9(a) shows the estimation error variance vs. the SNR under AWGN channel with CFO of 5 GHz. Note that for the proposed data-aided joint timing and frequency synchronization algorithm, when estimating the integral part of CFO, we utilize the method in Ref. [13], by inserting a pilot tone whose power is 5 times higher than the average power of the signal. The integral part can be estimated by just calculating the shift positions of the pilot tone. It can be seen that the ZSP method performs the worst, because the step size is only 0.01, which may be not large enough to achieve accurate CFO estimation. Another reason is that the ZSP method utilizes only one OFDM symbol for estimation, and the number of zero-subcarriers may be not large enough to get accurate results. The modified ZSP (MZSP) method performs the best when the SNR is larger than or equal to 25 dB, and the improvement compared with Schmidl's method is around half an order, and more than one order compared with ZSP method, at 25 dB SNR. Moreover, we also show the CFO estimation performance of the proposed DA method in Fig. 9(a). It can be easily observed that the proposed DA method outperforms Schmidl's method and ZSP method. At the estimation error variance of 10^{-5}, the SNR gain of the proposed DA method is almost 5 dB compared with that of Schmidl's method. When the SNR is below 25 dB, the proposed DA method shows best performance. Note that the CFO estimation accuracy of the ZSP and MZSP method can be improved by reducing the step size, or increasing the number of zero-subcarriers or number of OFDM symbol for power average.

Figure 9(b) investigates the CD tolerance of the proposed ZSP, MZSP, DA and Schmidl's method at 15 dB SNR. The dispersion factor in this simulation is 17 ps/nm/km. As can be seen in Fig. 9(b), the proposed DA method performs the best when transmit through a short distance. When the distance is larger than 0.5 km, the MZSP method performs best. This is because the MZSP method takes the power average through a series of OFDM symbols, which actually filters the noise and increase the SNR correspondingly. The proposed DA method outperforms the Schmidl's method when the transmission distance is shorter than 10 km, and performs worse when the distance is longer than 10 km. The appearance of CD will cause signal distortions. Different from Schmidl's method that contains two identical halves, the training

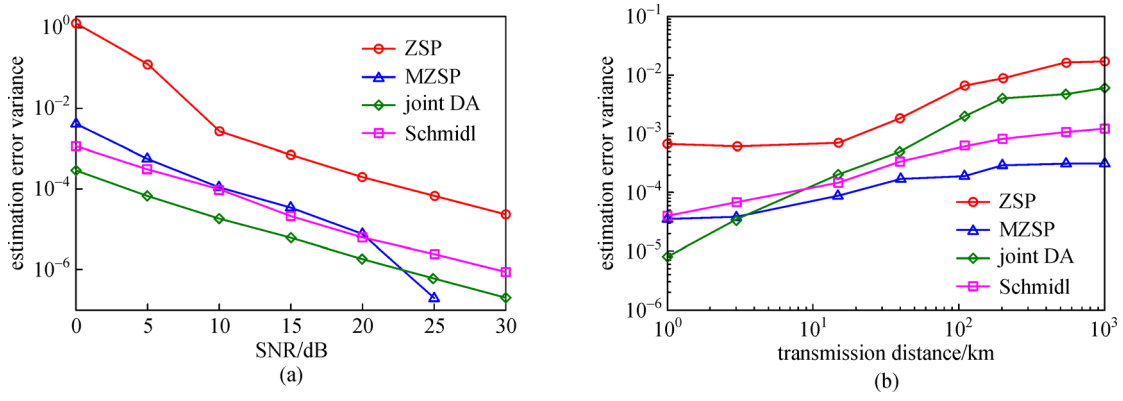

Fig. 9 (a) Estimation error variance vs. SNR under AWGN channel with CFO of 5 GHz; (b) estimation error variance vs. the transmission distance, with the CFO of 5 GHz, CLW of 100 kHz and dispersion parameter is 17 ps/nm/km, at 15 dB SNR

symbol of the proposed DA method uses the conjugate symmetric sequence which will be distorted more severely with the existence of CD. This is why the proposed DA method performs worse than Schmidl's method when transmitting a long distance.

The selection of the DA and BL method depends on certain requirements. For short distance transmission, the proposed DA method is a good choice, since it not only can achieve timing and frequency synchronization jointly with only one OFDM symbol, but also has better performance than the conventional algorithms. If a much better performance is required, with full transmission data rate, the proposed blind method is a better choice. Actually, the proposed DA method requires a training symbol for joint timing and frequency synchronization, and to achieve accurate CFO estimation performance, the computational complexity of the proposed BL method is high. Thus, the selection of the DA and BL method is actually a balance between the transmission efficiency, estimation accuracy and complexity.

6 Conclusions

In this paper, we present joint timing and frequency synchronization algorithms for CO-OFDM systems. We review our timing synchronization algorithm, and both the data-aided and blind algorithms for CFO estimation. We first present the special structure for the OFDM training symbol and design the timing metric for timing estimation. Furthermore, we present our data-aided CFO estimation algorithm which utilizes the same training symbol structure to estimate the CFO. Then a blind ZSP-based algorithm is shown, and a modified method is subsequently demonstrated to further improve the CFO estimation performance, to have a better tolerance to both AWGN and CD.

The effectiveness of joint timing and synchronization methods is demonstrated through both simulations and experiments. Both timing synchronization with DA CFO estimation and BL CFO estimation algorithms utilize only one OFDM symbol which ensures the effective transmission bit rate, but with the reduction of spectral efficiency. The results show that the proposed timing synchronization method can achieve better timing estimation performance compared with other conventional methods, and the DA CFO estimation method is feasible and stable. Moreover, we also investigate the CFO estimation performance of the ZSP and modified ZSP methods, and compare them with a conventional method. It shows that the modified ZSP algorithm has strong tolerance to the AWGN and CD, which is promising for applications.

Acknowledgements The authors would like to thank the supports of Grants 61501313, 61571316 and 61302112 from NSFC and Grant 1-ZE5K from the Hong Kong Polytechnic University.

References

1. Shieh W, Djordjevic I. OFDM for Optical Communications. Burlington: Academic Press, 2009
2. Shieh W, Athaudage C. Coherent optical orthogonal frequency division multiplexing. Electronics Letters, 2006, 42(10): 587–589
3. Hara S, Prasad R. Multicarrier Techniques for 4G Mobile Communiations. Norwood, MA: Artech House, 2003
4. Pollet T, Van Bladel M, Moeneclaey M. BER sensitivity of OFDM systems to carrier frequency offset and wiener phase noise. IEEE Transactions on Communications, 1995, 43(2–4): 191–193
5. Abdzadeh-Ziabari H, Zhu W P, Swamy M N S. Joint maximum likelihood timing, frequency offset, and doubly selective channel estiamtion for OFDM systems. IEEE Transactions on Vehicular Technology, 2018, 67(3): 2787–2791
6. Lin D D, Pacheco R A, Lim T J, Hatzinakos D. Joint estimation of channel response, frequency offset, and phase noise in OFDM. IEEE Transactions on Signal Processing, 2006, 54(9): 3542–3554
7. van de Beek J J, Sandell M, Borjesson P O. ML estimation of time and frequency offset in OFDM systems. IEEE Transactions on Signal Processing, 1997, 45(7): 1800–1805
8. Schmidl T M, Cox D C. Robust frequency and timing synchronization for OFDM. IEEE Transactions on Communications, 1997, 45 (12): 1613–1621
9. Minn H, Zeng M, Bhargava V K. On timing offset estimation for OFDM systems. IEEE Communications Letters, 2000, 4(7): 242–244
10. Park B, Cheon H, Kang C, Hong D. A novel timing estimation method for OFDM systems. IEEE Communications Letters, 2003, 7 (5): 239–241
11. Du X, Zhang J, Xu Z, Yu C. A novel timing estimation method for coherent optical OFDM systems. In: Proceedings of Asia Communications and Photonics Conference. Optical Society of America, 2015, paper AS4F. 5
12. Du X, Zhang J, Li Y, Yu C, Kam P Y. Efficient joint timing and frequency synchronization algorithm for coherent optical OFDM systems. Optics Express, 2016, 24(17): 19969–19977
13. Cao S, Zhang S, Yu C, Kam P Y. Full-range pilot-assisted frequency offset estimation for OFDM systems. In: Proceedings of Optical Fiber Communication Conference/National Fiber Optic Engineers Conference. Optical Society of America, 2013, paper JW2A. 53
14. Zhou X, Long K, Li R, Yang X, Zhang Z. A simple and efficient frequency offset estimation algorithm for high-speed coherent optical OFDM systems. Optics Express, 2012, 20(7): 7350–7361
15. Wu J, Tang M, Xu L, Zhu S, Cheng J, Feng Z, Zhang L, Wang X, Lin R, Deng L, Fu S, Shum P P, Liu D. A robust and efficient frequency offset correction algorithm with experimental verification for coherent optical OFDM system. Journal of Lightwave Technology, 2015, 33(18): 3801–3807
16. Kim D K, Do S H, Lee H K, Choi H J. Performance evaluations of the frequency detectors for orthogonal frequency division multiplexing. IEEE Transactions on Consumer Electronics, 1997, 43(3): 776–783
17. Huang Y J, Wei S W. Modified guard band power detection for coarse carrier frequency offset receovery in OFDM system. Wireless

Personal Communications, 2008, 45(2): 163–173
18. Du X, Zhang J, Yu C, Kam P Y. Blind carrier frequency offset estimation for coherent optical OFDM systems. In: Proceedings of Advanced Photonics (IPR, NOMA, Sensors, Networks, SPPCom, SOF). Optical Society of America, 2016, paper SpW2G.3
19. Zhu P, Li J, Zhao H, Tian Y, Chen Y, Wu Z, Chen Z, He Y. An iterative frequency offset estimation method for coherent optical OFDM system. IEEE Photonics Technology Letters, 2017, 29(11): 877–880
20. Jignesh J, Corcoran B, Zhu C, Lowery A. Simple optoelectronic frequency-offset estimator for coherent optical OFDM. Optics Express, 2017, 25(25): 32161–32177

Dr. **Changyuan Yu** received his Ph.D. degree in Electrical Engineering from the University of Southern California, USA in 2005. He was a visiting researcher at NEC Labs America in Princeton, USA in 2005. He then joined the faculty of National University of Singapore (NUS) in 12/2005, where he served as the founding leader of Photonic System Research Group in Department of Electrical and Computer Engineering. He was also a joint senior scientist with Institute for Infocomm Research (I2R), Agency for Science, Technology and Research (A*STAR) in Singapore. In 12/2015, he joined The Hong Kong Polytechnic University as an associate professor in Department of Electronic and Information Engineering. And he also continues as an adjunct associate professor of NUS. His research focuses on photonic devices, subsystems, optical fiber communication and sensor systems, and biomedical instruments. As the PI/co-PI, he secured over 5 million US dollars grants, and supervised 10 postdocs and 20 PhD students. He has authored/co-authored 1 US patent, 6 book chapters, 400 + journal and conference papers (75 invited, including OFC2012 in USA). His group won 6 best paper awards in conferences and the championship in biomedical area in the 3rd China Innovation and Entrepreneurship Competition in 2014.